

(3) for any numerical calculation of $\partial T_L/\partial P$ for Nb_3Sn . A similar calculation on dT_C/dP , including the interband charge-transfer effect, can be done.

In conclusion, we have observed for the first time pressure-enhanced lattice transformation in a high- T_C superconductor. The opposite pressure effects on T_L and T_C of Nb_3Sn and V_3Si can be explained in terms of the WLF model by taking into account the pressure-induced interband charge transfer. Previous atmospheric results on T_L and T_C of doped Nb_3Sn samples were discussed and an expression for dT_L/dP was also obtained.

The author would like to thank Dr. L. R. Testardi for stimulating discussions throughout this work and Dr. L. J. Vieland for the sample. Valuable discussions with Dr. C. S. Ting and Professor G. R. Barsch are gratefully acknowledged.

*Research supported in part by National Science Foundation Grant No. GH-40866 and by the Research Corporation.

¹For a review see L. R. Testardi, in *Physical Acoustics*, edited by W. P. Mason and R. N. Thurston (Academic, New York, 1974), Vol. X.

²C. W. Chu and T. F. Smith, *Bull. Amer. Phys. Soc.* **17**, 311 (1972); T. F. Smith, R. N. Shelton, A. C. Lawson, and C. W. Chu, to be published.

³T. F. Smith, R. N. Shelton, and A. C. Lawson, *J. Phys. F: Metal Phys.* **3**, 2157 (1973).

⁴C. W. Chu and L. R. Testardi, *Phys. Rev. Lett.* **32**, 766 (1974).

⁵H. Neubauer, *Z. Phys.* **266**, 211 (1969); T. F. Smith, *J. Low Temp. Phys.* **6**, 171 (1972).

⁶C. W. Chu and G. S. Knapp, *Phys. Lett.* **46A**, 33 (1973).

⁷A. Sawaoka and N. Kawai, *Jpn. J. Appl. Phys.* **9**, 353 (1970).

⁸R. Mailfert, B. W. Batterman, and J. J. Hanak, *Phys. Status Solidi* **32**, K67 (1969); G. Shirane and J. D. Axe, *Phys. Rev. B* **4**, 2957 (1971).

⁹L. J. Vieland and A. W. Wicklund, *Solid State Commun.* **7**, 37 (1969).

¹⁰C. W. Chu and L. J. Vieland, to be published.

¹¹For a review see M. Weger and I. B. Goldberg, in *Solid State Physics*, edited by H. Ehrenreich, F. Seitz, and D. Turnbull (Academic, New York, 1974), Vol. 28.

¹²J. Labbé, S. Barišić, and J. Friedel, *Phys. Rev. Lett.* **19**, 1039 (1967); J. Labbé, *Phys. Rev.* **172**, 451 (1968).

¹³P. F. Carcia, G. R. Barsch, and L. R. Testardi, *Phys. Rev. Lett.* **27**, 944 (1971); P. F. Carcia and G. R. Barsch, to be published.

¹⁴C. S. Ting and A. K. Ganguly, *Phys. Rev. B* **9**, 2781 (1974); G. R. Barsch and D. A. Rogowski, to be published.

¹⁵T. F. Smith, *Phys. Rev. Lett.* **25**, 1483 (1970);

H. Neubauer, *Z. Phys.* **226**, 211 (1969).

¹⁶S. Huang and C. W. Chu, *Bull. Amer. Phys. Soc.* **19**, 228 (1974), and to be published.

¹⁷L. J. Vieland and A. W. Wicklund, *Phys. Lett.* **34A**, 43 (1971).

¹⁸S. J. Williamson, H. Fung, and C. S. Ting, *Phys. Rev. Lett.* **32**, 9 (1974).

¹⁹L. J. Vieland, *J. Phys. Chem. Solids* **31**, 1449 (1970).

Variation of T_C with Electron-per-Atom Ratio in Superconducting Transition Metals and Their Alloys

I. R. Gomersall and B. L. Gyorffy

H. H. Wills Physics Laboratory, Royal Fort, Bristol BS8 1TL, United Kingdom

(Received 17 June 1974)

A microscopic explanation is given for the variation of the superconducting transition temperature T_C with the electron-per-atom ratio in transition metals and their alloys.

As was first noted by Matthias,¹ if one plots the superconducting transition temperature T_C against the electron-per-atom ratio \bar{z} for various metals, one obtains a two-peaked curve with maxima at $\bar{z} \approx 4.5$ and at $\bar{z} \approx 6.5$ and a deep minimum at $\bar{z} \approx 5.5$. This is the most consistently obeyed empirical rule relating T_C to a normal-state property and it has often proved to be of practical significance in searches for high- T_C materials.² The purpose of this note is to provide a first-

principles understanding of how such behavior arises as a consequence of interactions between electrons and phonons in a metal.

According to McMillan's solution of the strong-coupling gap equation³

$$T_C = \frac{\langle \omega \rangle}{1.2} \exp \left\{ - \frac{1.04(1+\lambda)}{\lambda - \mu^*(1+0.62\lambda)} \right\}, \quad (1)$$

where μ^* is an electron-electron interaction parameter which may be set equal to 0.13 for all

the transition metals, $\langle \omega \rangle$ is a suitably averaged phonon frequency defined by Dynes,⁴ and λ is the mass enhancement factor. Furthermore, it is useful to write

$$\lambda = (M \langle \omega^2 \rangle)^{-1} n(\epsilon_F) \langle I^2 \rangle, \quad (2)$$

where M is the ionic mass, $n(\epsilon_F)$ is the density of states at the Fermi energy ϵ_F , $\langle \omega^2 \rangle$ is an average of phonon frequencies as defined by McMillan,³ and $\langle I^2 \rangle$ is the average of the electron-phonon matrix elements over the Fermi surface. To a good approximation³ $\langle \omega^2 \rangle = \int d\omega \omega F(\omega) / \int d\omega \omega^{-1} F(\omega)$ and $\langle \omega \rangle = 1 / \int d\omega \omega^{-1} F(\omega)$,⁴ where $F(\omega)$ is the phonon density of states, and

$$\langle I^2 \rangle = \frac{2M}{N n^2(\epsilon_F)} \int \frac{d^3 k}{(2\pi)^3} \int \frac{d^3 k'}{(2\pi)^3} \sum_{\nu} \Omega_{\vec{k}-\vec{k}', \nu} |g_{\vec{k}, \vec{k}'; \nu}|^2 \delta(\epsilon_{\vec{k}}) \delta(\epsilon_{\vec{k}'}),$$

where N is the number of atoms per unit volume, the $\Omega_{\vec{k}-\vec{k}', \nu}$'s are the bare phonon frequencies unrenormalized by their interaction with the electrons, $\epsilon_{\vec{k}}$ and $\epsilon_{\vec{k}'}$ are Bloch-state energies measured from ϵ_F , and $g_{\vec{k}, \vec{k}'; \nu}$ is the matrix element of the electron-phonon interaction which takes an electron from the state \vec{k} (denoting both wave number and band index) to the state \vec{k}' with the simultaneous emission or absorption of a phonon with wave number $\vec{q} = \vec{k} - \vec{k}'$ and mode index ν .

It is now well established that Eqs. (1) and (2) provide a good account of the variations of T_c if $n(\epsilon_F) \langle I^2 \rangle$ is calculated from first principles and both $\langle \omega^2 \rangle$ and $\langle \omega \rangle$ are estimated empirically.^{5,6} However, one notes with dismay that although λ depends explicitly on $n(\epsilon_F)$, which varies by an order of magnitude across the periodic table, the product $n(\epsilon_F) \langle I^2 \rangle$ turns out to be much the same for all transition metals.³ Hence, in order to have a real understanding of the trends in T_c , we need a first-principles theory of $\langle \omega^2 \rangle$.

Consider a system of interacting electrons and phonons described by the Hamiltonian

$$H = \sum_{\vec{k}} \epsilon_{\vec{k}} C_{\vec{k}}^{\dagger} C_{\vec{k}} + \sum_{\vec{q}, \nu} \Omega_{\vec{q}, \nu} (b_{\vec{q}, \nu}^{\dagger} b_{\vec{q}, \nu} + \frac{1}{2}) + \sum_{\vec{k}, \vec{q}, \nu} g_{\vec{k}, \vec{k}+\vec{q}; \nu} C_{\vec{k}}^{\dagger} C_{\vec{k}+\vec{q}} (b_{\vec{q}, \nu} + b_{\vec{q}, \nu}^{\dagger}), \quad (4)$$

where $C_{\vec{k}}^{\dagger}$ and $C_{\vec{k}}$, respectively, create and annihilate Bloch electrons; $b_{\vec{q}, \nu}^{\dagger}$ and $b_{\vec{q}, \nu}$ do the same for bare phonons, and all other symbols have been defined previously. For one-electron states, we have in mind the results of a band-structure calculation based on an electron-ion potential constructed according to the Mattheiss prescription.⁷ Unlike pseudopotentials, such potentials include some electron-electron interactions, and we shall assume that no further screening is necessary. Similarly, for $\Omega_{\vec{q}, \nu}$ we do not take the bare plasma frequency of the ions. It is difficult to be more specific than that. A consistent prescription would be to construct the bare force constants from a neutral-atom interatomic potential calculated from the atomic charge densities. Fortunately, for the sake of the present discussion, it will suffice to assume that the $\Omega_{\vec{q}, \nu}$'s are the result of those direct interactions between ions which do not depend on the band structure. Finally, for $g_{\vec{k}, \vec{k}+\vec{q}; \nu}$ we take the rigid-ion prescription. We believe that such a description is appropriate to transition metals.

Because of the interaction between the electrons and phonons the bare force constants are softened and a convenient way of calculating the new frequencies $\omega_{\vec{q}, \nu}^{\pm}$ is to write⁸

$$\omega_{\vec{q}, \nu}^{\pm 2} = \Omega_{\vec{q}, \nu}^2 + 2\Omega_{\vec{q}, \nu} \text{Re} \Pi_{\nu}(\vec{q}; \omega = 0), \quad (5)$$

where $\Pi_{\nu}(\vec{q}; \omega)$ is the phonon self-energy and using the adiabatic approximation we set $\omega = 0$. We now approximate $\Pi_{\nu}(\vec{q}; \omega)$ by the first bubble diagram in its series expansion and write

$$\Pi_{\nu}(\vec{q}; \omega) = -2i \int (d\epsilon/2\pi) \sum_{\vec{k}} |g_{\vec{k}, \vec{k}+\vec{q}; \nu}|^2 G_0(\vec{k}; \epsilon) G_0(\vec{k}+\vec{q}; \epsilon + \omega), \quad (6)$$

where $G_0(\vec{k}; \epsilon)$ is the usual time-ordered Green's function for the unperturbed Bloch electrons. Together with the appropriate definitions, Eqs. (5) and (6) constitute the microscopic lattice dynamics we seek. This theory is still intractable; therefore, we make two further approximations.

First, we assume that, to the accuracy we need, we can replace $\langle \omega^2 \rangle_{\text{McM}}$ by $\langle \omega^2 \rangle_0 \equiv (3N)^{-1} \sum_{\vec{q}, \nu} \omega_{\vec{q}, \nu}^2$ and take $\langle \omega \rangle$ to be $\langle \omega^2 \rangle_0 / 1.1$.

Second, in calculating

$$\langle \omega^2 \rangle_0 = \langle \Omega^2 \rangle_0 + (3N)^{-1} \sum_{\vec{q}, \nu} 2\Omega_{\vec{q}, \nu} \text{Re} \Pi_{\nu}(\vec{q}; \omega = 0), \quad (7)$$

where $\langle \Omega^2 \rangle_0 \equiv (3N)^{-1} \sum_{\vec{q}, \nu} \Omega_{\vec{q}, \nu}^2$ and the relation was obtained from Eq. (5) by summing over \vec{q} and ν on both sides, we evaluate $\text{Re}\Pi_{\nu}(\vec{q}; 0)$ in the following manner. We use the Kramers-Kronig relation, i.e.,

$$\text{Re}\Pi_{\nu}(\vec{q}; 0) = -2 \int_0^{\infty} d\omega \Pi^{-1} \omega^{-1} \text{Im}\Pi_{\nu}(\vec{q}; \omega)$$

and note that, quite generally, $\text{Im}\Pi_{\nu}(\vec{q}, \omega)$ starts linearly with ω from the origin and cuts off at some frequency ω_c . This suggests that we approximate $\text{Im}\Pi_{\nu}(\vec{q}; \omega)$ by $\omega \partial \text{Im}\Pi_{\nu}(\vec{q}; \omega) / \partial \omega |_{\omega=0}$ and take

$$\text{Re}\Pi_{\nu}(\vec{q}, 0) = - (2/\pi) \omega_c \left. \frac{\partial \text{Im}\Pi_{\nu}(\vec{q}; \omega)}{\partial \omega} \right|_{\omega=0} \tag{8}$$

We now substitute Eq. (6) into Eq. (8) and use the resulting expression for $\text{Re}\Pi_{\nu}(\vec{q}, 0)$ in Eq. (7) to obtain

$$\langle \omega^2 \rangle_0 = \langle \Omega^2 \rangle_0 - \frac{8\omega_c}{3N} \sum_{\nu} \int \frac{d^3k}{(2\pi)^3} \int \frac{d^3k'}{(2\pi)^3} \Omega_{\vec{k}-\vec{k}', \nu} |g_{\vec{k}, \vec{k}'; \nu}|^2 \delta(\epsilon_{\vec{k}}) \delta(\epsilon_{\vec{k}'}), \tag{9}$$

where the energies $\epsilon_{\vec{k}}$ and $\epsilon_{\vec{k}'}$ are measured from the Fermi energy, ϵ_F . Some details of the entirely straightforward manipulations leading to Eq. (9), and a discussion of the validity of the above approximations, will be given elsewhere.

Observe now that the second term on the right-hand side of Eq. (9) is proportional to $n(\epsilon_F) \langle I^2 \rangle$ given in Eq. (3). Thus, by estimating the cut of frequency ω_c from a free-electron model to be $\frac{3}{5} \epsilon_F$, we may summarize the above discussion by writing

$$\langle \omega^2 \rangle \cong \langle \omega^2 \rangle_0 \cong \langle \Omega^2 \rangle_0 - \frac{4}{5} \epsilon_F n(\epsilon_F) M^{-1} [n(\epsilon_F) \langle I^2 \rangle]. \tag{10}$$

From a technical point of view this is our main result. It shows how $\langle \omega^2 \rangle$ depends on the band structure and the Fermi energy. Here, however, we are more interested in what the softening of the mode does to λ and therefore T_c . From Eqs. (2) and (10) we have that

$$\lambda = \lambda_0 [1 - \frac{4}{5} \epsilon_F n(\epsilon_F) \lambda_0]^{-1}, \tag{11}$$

where $\lambda_0 = n(\epsilon_F) \langle I^2 \rangle / M \langle \Omega^2 \rangle_0$, i.e., the electron mass enhancement due to the unrenormalized phonons. As we expect $n(\epsilon_F) \langle I^2 \rangle$ and $\langle \Omega^2 \rangle_0$ to be roughly the same for all the transition metals, we assume that λ_0 is a constant in \mathfrak{z} . In Fig. 1

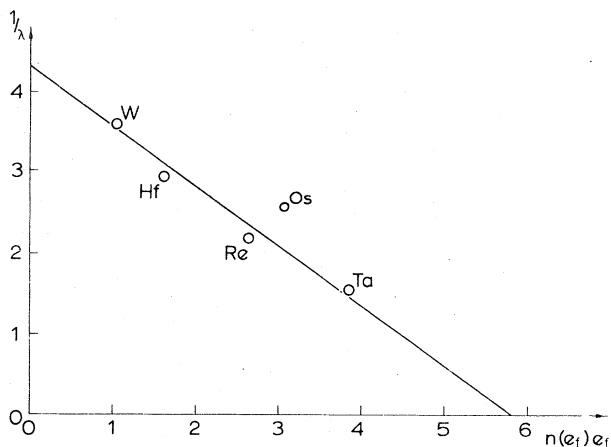


FIG. 1. Empirical values of λ^{-1} plotted as a function of $\epsilon_F n(\epsilon_F)$, where ϵ_F is measured relative to the bottom of the conduction band, for the 5-d transition metals.

we show a plot of empirical values for λ^{-1} versus $\epsilon_F n(\epsilon_F)$ for a number of transition metals. For $n(\epsilon_F)$ we used the empirical values of McMillan³ and ϵ_F was determined by the rigid-band assumption and Mattheiss's W_1 band structure calculation for tungsten⁹; see Fig. 2. It is gratifying that we obtain a rather good straight line. Surprisingly, the slope is roughly $\frac{4}{5}$, as would follow from Eq. (11). From the intercept we estimate $\lambda_0^{-1} = 4.3$.

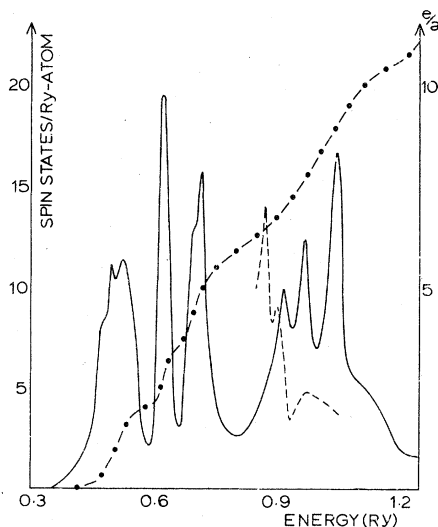


FIG. 2. The density of states of W (solid line) and Re (dashed line), and the integrated density of states of W (dash-dotted).

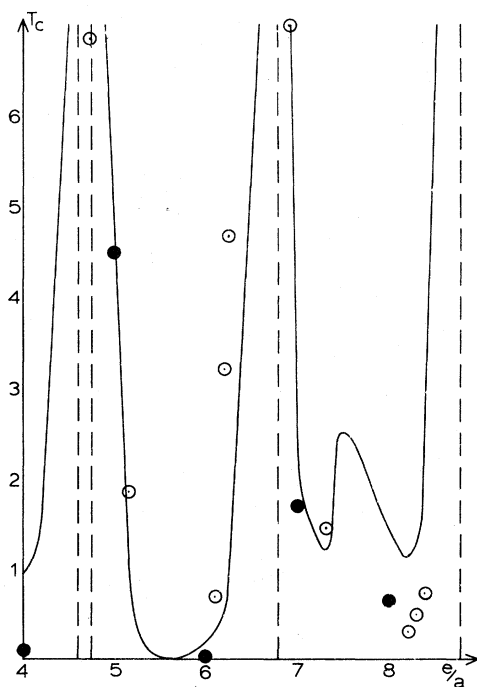


FIG. 3. The superconducting transition temperature given by the present theory, as explained in the text, plotted as a function of \bar{z} (solid line). The closed circles correspond to experimentally observed transition temperatures for pure metals and the open circles are those for alloys.

Using this value for λ_0 and the density of states of W,⁹ together with the rigid-band idea, we have calculated λ and then, from Eq. (1), T_c for $4.7 \lesssim \bar{z} \lesssim 6.8$. The results are shown in the middle portion of Fig. 3. As a consequence of ϵ_F moving into the deep valley separating the bonding from the antibonding peaks of the d band, around \bar{z} appropriate to W, we get a minimum in T_c for an approximately half-filled band, in a remarkably good agreement with experiments. As ϵ_F moves out of this valley towards either the bonding (low-energy) or antibonding (high-energy) peaks—see Fig. 2— T_c rises until $\langle \omega^2 \rangle_0 = \langle \Omega^2 \rangle_0 [1 - (\frac{2}{3})\epsilon_F n(\epsilon_F)\lambda_0]$ becomes negative at $\bar{z} = 4.7$ and at $\bar{z} = 6.8$. This suggests that for values of $n(\epsilon_F)$ higher than the ones corresponding to these singular points the bcc lattice is no longer stable. Indeed, we find that the transition metals with $\bar{z} = 4$ and $\bar{z} = 7$ form hcp lattices. This view is strongly supported if we look at the density of states of Re shown in Fig. 2. While for bcc W, $\bar{z} = 6.7$ corresponds to an ϵ_F moving towards a peak in the density of states making $n(\epsilon_F)$ very large, in hcp Re¹⁰ for the same \bar{z} , one is over the antibonding peak and,

for further filling of the d band, $n(\epsilon_F)$ is decreasing. For $\bar{z} \leq 4.7$ and $\bar{z} \geq 6.8$ we have calculated T_c using the density of states for Re in the same way as we have used that of W previously. The results are shown in Fig. 3.

Beyond $\bar{z} \cong 8$ the rise in T_c again corresponds to an approaching lattice instability. At $\bar{z} \cong 8.8$, $\langle \omega^2 \rangle - 0$. Significantly, Ir with $\bar{z} = 9$ crystallizes in an fcc structure. Unfortunately, Eq. (12) does not predict λ for Ir correctly. Presumably, λ_0 is not the same for the fcc transition metals as for the others.

Thus Eq. (11) together with Eq. (1) gives a good quantitative account of the variation of T_c with \bar{z} for the hcp and bcc transition metals across the second series with a single empirical parameter λ_0 . In addition, the theory predicts correctly the changes in crystal structure as a function of \bar{z} for the metals in question. We find that for certain values of \bar{z} which correspond to large density of states at the Fermi energy, the lattice changes its structure in order to reduce the strength of the electron-phonon coupling. Also, we note that T_c is larger near such instabilities. Matthias reached similar conclusions on empirical grounds.²

For random alloys one is tempted to replace $n(\epsilon_F)$ in Eq. (11) by the configurationally averaged density of states. If one accepts the rigid-band model,¹¹ the full line in Fig. 3 can be taken as the prediction for the appropriate alloy. The agreement is again good. Particularly encouraging is the rise of T_c in OsIr alloys. Clearly our theory would predict a further rise if this alloy can be made to form with $\bar{z} \geq 8.4$ in hexagonal solid solution. The peak at $\bar{z} \cong 7.5$ is due to a small but definite hump in the density of states of Re. This effect might also be observable.

We would like to thank Dr. P. B. Allen and Dr. W. E. Pickett for a very helpful discussion.

¹B. T. Matthias, Phys. Rev. **97**, 74 (1955).

²B. T. Matthias, in *Superconductivity in d- and f-Band Metals* AIP Conference Proceedings No. 4, edited by D. H. Douglass, Jr. (American Institute of Physics, New York, 1972), p. 367.

³W. L. McMillan, Phys. Rev. **167**, 331 (1968).

⁴R. C. Dynes, Solid State Commun. **10**, 615 (1972).

⁵P. B. Allen and M. L. Cohen, Phys. Rev. **187**, 525 (1969).

⁶R. Evans, G. Gaspari, and B. L. Gyorffy, J. Phys. F: Metal Phys. **3**, 39 (1973).

⁷L. F. Mattheiss, Phys. Rev. **133**, A1399 (1964).
⁸A. A. Abrikosov, L. P. Gorkov, and I. Ye. Dzyaloshinskii, *Quantum Field Theory Methods in Statistical Physics* (Pergamon, New York, 1965).

⁹L. F. Mattheiss, Phys. Rev. **139**, A1893 (1965).
¹⁰L. F. Mattheiss, Phys. Rev. **151**, 450 (1966).
¹¹G. M. Stocks, R. W. Williams, and J. S. Faulkner, Phys. Rev. B **4**, 2412 (1971).

Photoemission Final-State Spectroscopy Applied to KCl†

G. J. Lapeyre, J. Anderson, P. L. Gobby, and J. A. Knapp

Montana State University, Bozeman, Montana 59715

(Received 28 May 1974)

A new method of taking uv photoemission data, employing synchrotron radiation, is described. The method has significant advantages for investigating final-state properties of interband transitions and for investigating many-body effects. Applying it to KCl, strong peaks in the conduction-band density of states are located at 9.7 and 12.6 eV. The data also suggest a probable interpretation of an optical-reflectance peak ($h\nu \approx 13$ eV) whose origin has been a matter of doubt.

This Letter reports a new mode of performing ultraviolet photoemission spectroscopy (UPS) with synchrotron radiation which conveniently provides data bearing directly on the final-state properties of interband transitions. Previously, UPS studies have obtained final-state properties by measuring sets of energy distribution curves (EDC's) and then analyzing peak amplitudes or peak positions as a function of photon energy $h\nu$.^{1,2} In principle, all the information available from an ordinary photoemission investigation of a substance is implicit in a family of EDC's measured at closely spaced $h\nu$ values. In practice, however, detailed amplitude differences in adjacent EDC's are difficult or impossible to determine, so that final-state UPS studies have been restricted in scope. As a result, the typical photoemission experiment has emphasized the initial-state properties of optical excitations.

The above limitations are ultimately traceable to constraints imposed by the nature of the radiation source: i.e., a narrow or discontinuous spectrum. Synchrotron radiation, however, possesses a broad smooth spectrum and it has been possible to exploit this quality in certain experimental adaptations, as described below, which render the desired information much more accessible and conspicuous.

The alkali halide KCl is selected for discussion because it has very strong final-state properties, making the relation between the new mode and the more familiar EDC mode easy to recognize. Further, KCl provides a good example of the utility of the new mode for studying certain many-body effects. The data are examined for evidence of the two-electron excitation mechanism proposed

by DeVreese *et al.*,³ and no evidence is found to support the proposal. The data do, however, show a feature which may be due to an excitonic resonance associated with the very strong *d*-like states in the conduction bands.

The emission data are obtained from KCl films deposited on Au in ultrahigh vacuum—about 270 Å thick for the data shown. The experimental arrangement is outlined by Baer and Lapeyre⁴ and Lapeyre *et al.*⁴ Synchrotron radiation from the University of Wisconsin storage ring was used as the excitation source, and the spectral dependence of its intensity was obtained from sodium salicylate fluorescence measurements.

To introduce the new mode of performing UPS experiments, we first present a set of EDC's in Fig. 1,⁵ arranged to demonstrate that the number of electrons photoemitted with final-state energy E_f is a two-variable function $N(E_f, h\nu)$ which can be viewed in three dimensions as a surface—the emission surface. The reference energy is the valence-band maximum and the threshold (vacuum level) is 8.6 ± 0.2 eV. In this picture the EDC corresponds to a scan along a constant- $h\nu$ line and is denoted by $N(E_f; h\nu \text{ fixed})$. Measurement of a family of EDC's is the classic mode for determining the properties of the emission surface. The peak which occurs at the far right of each curve is due to electrons emitted from the valence bands (VB) without energy loss—the VB primaries—and the width of the peak represents the width of the VB's (2.5 ± 0.2 eV). The balance of the electrons, emitted at lower energies, form the secondaries.

The new mode scans along a different section of the emission surface corresponding to the